Numerical modelling of liquid droplet dynamics in microgravity



2011 J. Phys.: Conf. Ser. 327 012027

(http://iopscience.iop.org/1742-6596/327/1/012027)

Journal of Physics: Conference Series **327** (2011) 012027 doi:10.1088/1742-6596/327/1/012027

# Numerical Modelling of Liquid Droplet Dynamics in Microgravity

**S. Easter, V. Bojarevics, K. Pericleous**

University of Greenwich, Park Row, London SE10 9LS, UK

V.Bojarevics@gre.ac.uk

**Abstract**. Microgravity provides ideal experimental conditions for studying highly reactive and under-cooled materials where there is no contact between the sample and the other experimental apparatus. The non-contact conditions allow material properties to be measured from the oscillating liquid droplet response to perturbations. This work investigates the impact of a strong magnetic field on these measurement processes for weakly viscous, electrically conducting droplets. We present numerical results using an axisymmetric model that employs the pseudo-spectral collocation method and a recently developed 3D model. Both numerical models have been developed to solve the equations describing the coupled electromagnetic and fluid flow processes. The models represent the changing surface shape that results from the interaction between forces inside the droplet and the surface tension imposed boundary conditions. The models are used to examine the liquid droplet dynamics in a strong DC magnetic field. In each case the surface shape is decomposed into a superposition of spherical harmonic modes. The oscillation of the individual mode coefficients is then analysed to determine the oscillation frequencies and damping rates that are then compared to the low amplitude solutions predicted by the published analytical asymptotic theory.

## 1. Introduction

The experiments with liquid metal droplets levitated in AC magnetic field show difficulties related to confinement instability and a need for complex correction functions to establish a correlation between the measurements and the droplet material properties [1-3]. A very intense internal fluid flow is visually observed, apparently being in the turbulent regime for earthbound conditions. The combination of AC and DC magnetic fields was recently recognised as an efficient tool for the electromagnetic processing of materials and for thermophysical property measurements without a contact to contaminating walls [4, 5]. The intense AC magnetic field required to produce levitation, along with the buoyancy and thermo-capillary forces, results in turbulent large-scale toroidal recirculation within the droplet, which prevents accurate measurements. The use of a homogenous DC magnetic field allows the toroidal flow to be damped. However the intense recirculation generates turbulence which could make the effective viscosity behave in a non-linear fashion depending on the DC and AC magnetic field intensity [5]. The flow in a typical droplet is approaching the conditions with laminar viscosity and heat transfer when a uniform DC magnetic field reaches about 4-5 T. Even a purely DC magnetic levitation, using para- and dia-magnetic properties of the materials, can be used for advanced material research [6, 7]. Due to the low values of magnetic susceptibility for typical liquid materials the fields are large (typically > 10 T), requiring superconducting coils with an associated cooling system. The vertical field gradient permits to compensate gravity along the central

axis, while the radial variation opposes motion of the droplet and acts to centre it on the axis for stable levitation. However, in practice a small vibration of the droplet as a whole remains even in carefully conducted experiments [7].

The oscillations in a high DC magnetic field are quite different for an electrically conducting droplet, like liquid metal. In a recent publication [8] an asymptotic solution for very high magnetic field shows damping of the even axisymmetric modes, but the odd modes are not damped or damped moderately. The asymptotic linear theory predicts a considerable shift of the oscillating droplet frequencies from the non-magnetic case. The transition of the droplet behavior from the low to high magnetic field is the subject of investigation in this paper. Numerical models of the flow coupled with the moving free surface give an insight to the dynamics and complexity of the events within levitated droplets of various sizes and magnetic field intensities. For simplicity we will restrict the study to uniform DC magnetic field, leaving the more general cases of realistic gradient fields, as in the solenoidal coils of superconducting magnets, for a future work.

## 2. Droplet oscillation mode decomposition

The general theoretical approach assumes that the free surface shape of the droplet is defined by a small deviation from a sphere of radius $R_0$. The surface position can be represented by:

$$r_s = R_0 \left[1 + S(\theta, \phi, t)\right]. \tag{1}$$

The function defining the deviation from a sphere (S) varies in time and space and can be represented in spherical polar coordinates as a series of spherical harmonics:

$$S(\theta, \phi, t) = \sum_{L=0}^{L=\infty} \sum_{M=0}^{M=L} A_L^M(t) P_L^M(\theta) \cos(M\phi) + A_L^{-M}(t) P_L^{-M}(\theta) \sin(-M\phi), \tag{2}$$

The $Y^0_0 = P^0_0$ mode is included to account for conservation of mass (volume). The time-dependent surface coefficients are assumed to be harmonic with exponential damping:

$$A_L^M(t) = \cos(\omega_L^M t) \exp(-\gamma_L^M t) \tag{3}$$

The mode dependent oscillation frequency and damping constants are generally derived by following a perturbation approach. The zero order result for the frequency was calculated by Rayleigh [9], and is given for a droplet with density $\rho$ and surface tension $\Gamma$ by:

$$\omega_L^M = \sqrt{\frac{L(L-1)(L+2)\Gamma}{\rho R_0^3}} \tag{4}$$

The zero order result for the damping coefficient for a droplet of viscosity $\nu$ was determined by Lamb [10]:

$$\gamma_L^M = \frac{(L-1)(2L+1)\nu}{R_0^2} \tag{5}$$

It is interesting to note that the zero order approximation for both the frequency and the damping constant are independent of the azimuthal number M. These formulae provide a good first approximation for low amplitude oscillations of droplets in microgravity conditions where the effects of any external forces used to position the droplet are negligible compared with surface tension and viscous forces. However it is worth noting that these formulae are restricted and are only valid in the limit that the amplitude of oscillation and also non-linear effects tend to zero. Modifications to these lowest order formulae have been derived by Tsamopoulos & Brown [11]; they showed that for 'moderate amplitude', the frequency decreases with increasing amplitude and that a coupling of the spherical harmonic modes appears at the second order.

Performing experiments in conditions where any external positioning forces are negligible (drop shafts, parabolic flights, space) is limited due to expense and also by the amount of time in which

experimental measurements can be made. The oscillating drop technique has been used in terrestrial conditions where the forces used to balance gravity and position the droplet are in the form of some sort of levitation, acoustic, aerodynamic, electromagnetic, or electrostatic. The use of a positioning field results in a more significant impact on the droplet dynamics and adjustments to the theoretical formulae are required. In the case of electromagnetic levitation correction formulae have been derived by Cummings & Blackburn [2], in which the external field is shown to remove the degeneracy of the L=2 modes resulting in a splitting of the frequency spectrum. Other levitation forces have also been considered by Suryanarayana & Bayazitoglu [3].

Perhaps the most promising method of confinement for conducting measurements using the oscillating droplet technique is diamagnetic levitation in a superconducting magnet. In this case the weak diamagnetic properties exhibited by many materials can be harnessed by a large magnetic field and used to balance the force of gravity without the more invasive Lorentz forces associated with AC electromagnetic levitation. The resulting total magnetic force on the droplet allows gravity to be compensated, although there is some variation in the force and a component that acts towards the axis, which means that it is a good approximation to microgravity conditions but not completely equivalent. Frequency measurements using the oscillating drop technique have been conducted for water droplets by Beaugnon et al. [6], where estimates were made as to the frequency modification due to the magnetic field. More recent experiments have been conducted by Hill & Eaves [7], in which a derivation of the frequency modifications due to the magnetic field are made and compared with the experimental results.

In a recent paper Priede [8], considers the effect of a constant high intensity magnetic field on the oscillation frequency and damping rate of an electrically conducting drop. The magnetic field is shown to significantly alter the dynamics of the droplet with some interesting results. There are two distinct cases; the longitudinal modes when (*L-M*) is odd and the transversal modes when (*L-M*) is even. The frequencies for the odd and even modes respectively are given by:

$$\omega_L^M = \sqrt{\frac{(L-1)(L+2)\Gamma}{\rho R_0^3}} \tag{6}$$

$$\omega_L^M = M\sqrt{\frac{(L-1)(L+2)}{L(L+1)-M^2}\frac{\Gamma}{\rho R_0^3}} \tag{7}$$

The damping constant consists of two components, damping due to the magnetic field $B_0$ and damping due to viscosity $\nu$. The damping contribution of the magnetic field for the odd and even modes respectively are given by:

$$\gamma_L^M = \frac{1}{6}(L-1)(L+2)\left((L-1)(L+2)+2M^2\right)\frac{\sigma B_0^2 R_0^3}{\Gamma} \tag{8}$$

$$\gamma_L^M = \frac{(L-1)(L+2)\left(L^2-M^2\right)\left((L+1)^2-M^2\right)\left(3L(L+1)-2M^2\right)}{6\left(L(L+1)-M^2\right)^2}\frac{\sigma B_0^2 R_0^3}{\Gamma} \tag{9}$$

The contribution to the damping constant due to viscous forces is given by:

$$\gamma_L^M = C_L^M \frac{\nu}{R_0^2} \tag{10}$$

Where ($C_L^M$) are coefficients determined by evaluation of an integral without a closed form solution. In this paper we are only concerned with the low order mode with coefficients as given in [8]:

$$C_2^1 = \frac{5}{2} \qquad C_2^2 = 5 \qquad C_3^0 = \frac{35}{3} \tag{11}$$

In the following section an outline is given of an axisymmetric and a 3D numerical model that will be used to investigate these effects. Following results are presented that demonstrate quantitatively the theoretical predictions and the gradual transition with the increase of the magnetic field.

## 3. Numerical Model

The 3D numerical model uses a grid point formulation of the spectral collocation method with the Chebyshev grid for the radial direction and Fourier in the angular directions. The model uses a coordinate transformation for the free surface, which allows the problem to be solved on a unit sphere. The equations solved by the numerical model are the momentum and mass conservation equations with the Poisson equation for the modified pressure, $P_{\mathrm{mod}} = P + \rho g z - \frac{\chi_v |B|^2}{2\mu_0}$ :

$$\frac{\partial \mathbf{V}}{\partial t} + (\mathbf{V}\cdot\nabla)\mathbf{V} = -\frac{1}{\rho}\nabla P_{\mathrm{mod}} + \nu\nabla\cdot\left(\nabla\mathbf{V} + \nabla\mathbf{V}^T\right) + \frac{\mathbf{J}\times\mathbf{B}}{\rho}; \quad \nabla\cdot\mathbf{V} = 0; \tag{12}$$

$$\frac{1}{\rho}\nabla^2 P_{\mathrm{mod}} = -\nabla\cdot\left[(\mathbf{V}\cdot\nabla)\mathbf{V} - \frac{1}{\rho}\mathbf{J}\times\mathbf{B}\right]. \tag{13}$$

The total force due to the magnetic field consists of two components, the Lorentz force due to the conducting properties, which is added to the momentum equations as a body force and the diamagnetic force, which is potential and is implemented in the model as boundary condition to the pressure equation along with the gravitational force, which is also potential. The full boundary conditions for the equations (12) and (13) relate the normal stress to the three forces (surface tension, gravity, and diamagnetic):

$$\mathbf{e_n}\cdot\Pi\cdot\mathbf{e_n} = \Gamma K + \rho g z - \frac{\chi_v |\mathbf{B}|^2}{2\mu_0}, \tag{14}$$

the continuity and the tangential stress conditions:

$$\nabla\cdot\mathbf{V} = 0, \tag{15}$$

$$\mathbf{e_n}\cdot\Pi\cdot\mathbf{e}_{\tau 1} = 0, \tag{16}$$

$$\mathbf{e_n}\cdot\Pi\cdot\mathbf{e}_{\tau 2} = 0, \tag{17}$$

where $\boldsymbol{e_n}, \boldsymbol{e}_{\tau 1}, \boldsymbol{e}_{\tau 2}$ are the unit vectors normal and tangential to the free surface, $\Pi$ is the stress tensor, $K$ is the surface curvature, and $\chi_v$ is the volumetric magnetic susceptibility.

The free surface shape is defined by its deviation from a sphere of radius $R_0$ by an amount $S$ given as a function of time and the angular coordinates:

$$r_s = R_0\left[1 + S(\theta,\phi,t)\right] \tag{18}$$

The new surface position at each time step is evaluated using the kinematic condition:

$$\frac{\partial r_s}{\partial t}\cdot\mathbf{e_n} = \mathbf{V}\cdot\mathbf{e_n}. \tag{19}$$

### 3.1. Electromagnetic Forces

The magnetic field from a solenoid is modelled as a superposition of the magnetic field generated by axisymmetric coil filaments of radius $a$. The axisymmetric magnetic field in cylindrical coordinates, $\mathbf{B}(r,0,z) = (B_r, 0, B_z)$, is obtained from the analytical formulae [12]:

$$B_r = \frac{\mu_0 I}{2\pi} \frac{z}{r\sqrt{(a+r)^2+z^2}} \left[ -K + \frac{a^2+r^2+z^2}{(a-r)^2+z^2} E \right] \tag{20}$$

$$B_z = \frac{\mu_0 I}{2\pi} \frac{1}{\sqrt{(a+r)^2+z^2}} \left[ K + \frac{a^2-r^2-z^2}{(a-r)^2+z^2} E \right] \tag{21}$$

Where, $a$ = coil radius, $I$ = electric current, $K$, $E$ are the complete elliptic integrals of the first and second kind respectively with argument, $k^2 = 4ar\left[(a+r)^2+z^2\right]^{-1}$.

The stable levitation conditions can be established by adjusting the electric current in the coils to form a minimum in the magneto-gravitational potential (per unit volume):

$$U_{vol} = \rho g z - \frac{\chi_v |\mathbf{B}|^2}{2\mu_0}. \tag{22}$$

The Lorentz body force requires an additional equation to be solved for the electric potential. The electric current density is given by:

$$\boldsymbol{J} = \sigma\left(-\nabla\phi_E + \boldsymbol{V}\times\boldsymbol{B}\right). \tag{23}$$

The equation for the electric potential is obtained from the charge conservation condition:

$$\nabla\cdot\boldsymbol{J} = 0. \tag{24}$$

Taking the divergence of the electric current density gives:

$$\nabla^2\phi_E = \nabla\cdot\left(\boldsymbol{V}\times\boldsymbol{B}\right). \tag{25}$$

This equation is solved subject to the boundary condition:

$$\boldsymbol{J}\cdot\boldsymbol{e_n} = 0. \tag{26}$$

The magnetic field in this paper is mostly prescribed as the constant field given in cylindrical coordinates by:

$$\boldsymbol{B}(r,\phi,z) = (0,0,B_0). \tag{27}$$

## 4. Results & Discussion

The following section contains the results of numerical simulations made using both the 2D axisymmetric [13] and 3D modes compared with theoretical asymptotic results from [8].

The material chosen for the numerical test cases is either molten silicon having the material property values for surface tension coefficient, density, kinematic viscosity, volumetric magnetic susceptibility, and conductivity, respectively: $\Gamma$ = 0.865 N m$^{-1}$, $\rho$ = 2510.0 Kg m$^{-3}$, $\nu$ = 3.75e-7 m$^2$ s$^{-1}$, $\chi_v$ = -4.2e-6, $\sigma$ = 1.3e6 S m$^{-1}$; or for the molten nickel: $\Gamma$ = 1.778 N m$^{-1}$, $\rho$ = 7995 Kg m$^{-3}$, $\nu$ = 6.2e-7 m$^2$ s$^{-1}$, $\chi_v$ = 1.6e-6, $\sigma$ = 1.18e6 S m$^{-1}$

### 4.1. Freely Oscillating Droplets, Axisymmetric Mode (2,0)

The first case considered is the axisymmetric mode $Y^0_2$ for the droplet of radius ($R_0$ = 5.0 mm), initial amplitude ($A^0_2$ = 0.01), and the velocity $\boldsymbol{V}$=0. The constant magnetic field has strength ($B_0$ = 2.5T). The initial amplitude corresponds to a polar deformation of 1% of the equilibrium droplet radius. A

small volume correction is applied in the form of a ($A^0_0$) coefficient, with the magnitude determined numerically.

Figure 1 shows the flow for a droplet moving in the ($Y^0_2$) mode with the external magnetic field. Maximum deformation occurs when t = 0, then monotonously decreases to reach the spherical shape as shown in the Figure 2 for various field magnitudes.

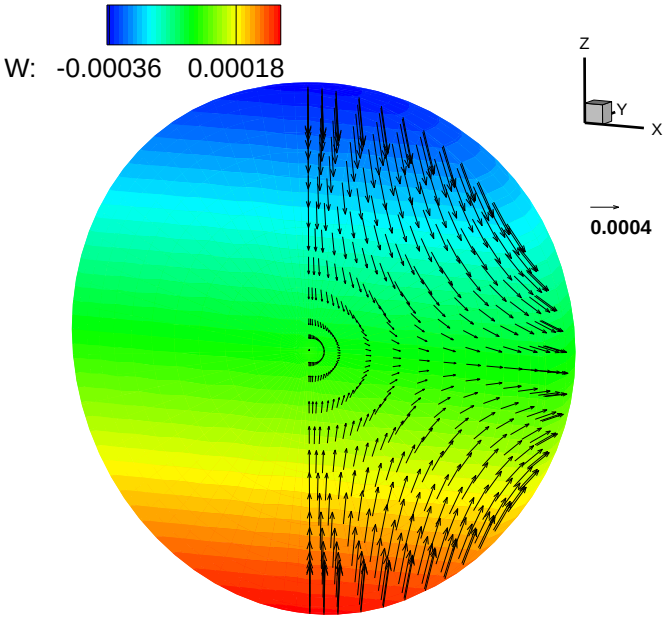


**Figure 1**. Oscillation mode (2,0), instantaneous velocity vectors and vertical velocity contours for Si droplet in 2.5 T magnetic field.

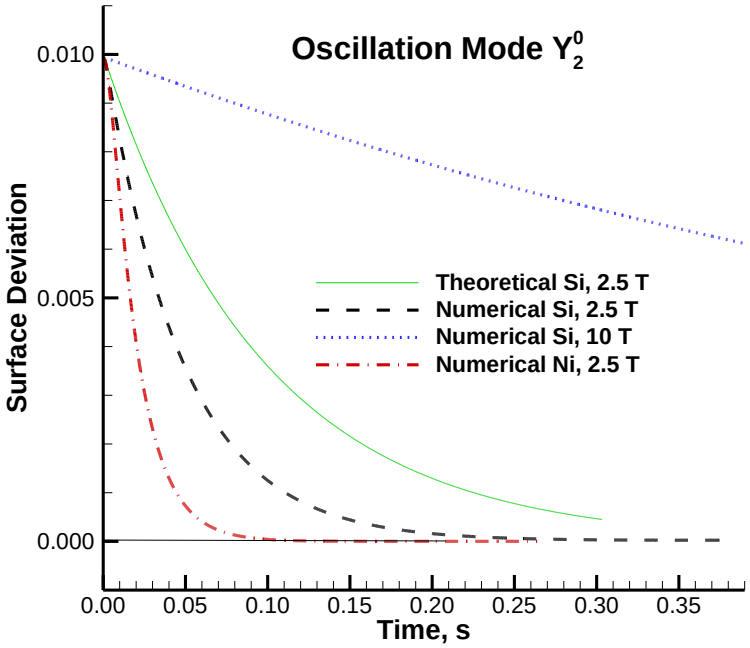


**Figure 2**. Surface deviation $(R_{top}-R_o)/R_o$ function evaluated at the top point for Si and Ni droplets in various magnetic fields.

Theoretical asymptotic analysis for high B shows that the mode is over-damped by the magnetic field, the oscillation frequency is zero and the magnetic damping constant is given by:

$$\gamma_2^0 = 12\frac{\sigma B_0^2 R_0^3}{\Gamma}. \quad (28)$$

The reason for this result is clear when observing the flow profile in the Figure 1. The flow component in radial direction u is perpendicular to the uniform magnetic field along the z-axis. Due to the symmetry of the flow it is not possible to satisfy mass continuity with a potential flow only in the z-direction. Figure 2 shows the results of a numerical simulation compared with the theoretical asymptotic result. In this case the numerical model shows a higher level of damping than the theoretical because the result (28) does not include the viscous damping for the axisymmetric mode at the finite value of the magnetic field. The numerical results show the dependence on the material properties and the field intensity. For the very high field (10 T) the damping leads to a very slow motion, and the droplet reaches the spherical shape in a considerably longer time than without field.

4.2. Freely Oscillating Droplets, Axisymmetric Mode (3,0)

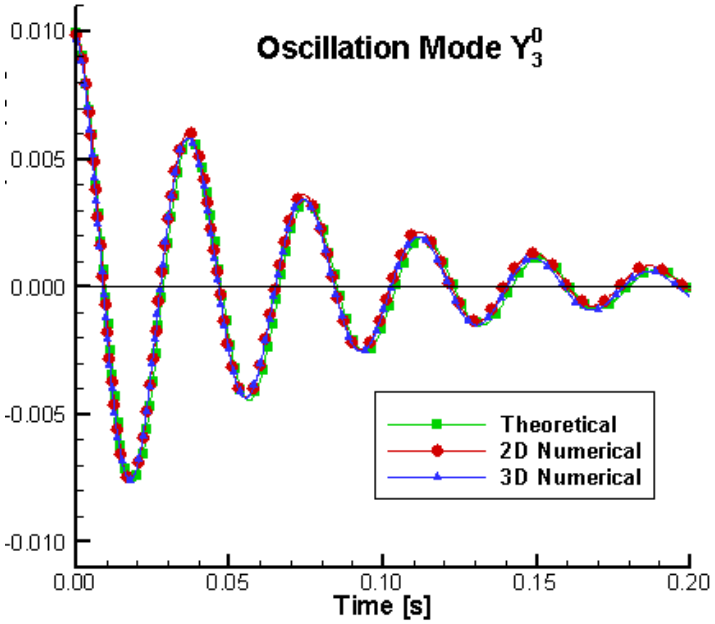


**Figure 3**. Surface deviation function, $(R_{top}-R_o)/R_o$ , evaluated at the top point for $B_o$ =2.5 T.

The next case considered is the axisymmetric mode ($Y^0_3$) droplet perturbation, the radius, amplitude, and magnetic field strength are all the same as in the previous case. An initial volume correction is again made to preserve the volume of the sphere with the radius $R_o$. Theoretical analysis shows that the oscillation frequency and the magnetic and viscous damping constants are given, respectively, by:

$$\omega_3^0 = \sqrt{\frac{10\Gamma}{\rho R_0^3}} \quad (29)$$

$$\gamma_3^0 = \frac{50}{3}\frac{\sigma B_0^2 R_0^3}{\Gamma} + \frac{35}{3}\frac{\nu}{R_0^2}. \quad (30)$$

Figure 3 shows the results of the numerical simulations with both the 2D and 3D modes compared with the theoretical result. There is reasonably good agreement with all 3 results.

Figure 4 shows a Ni droplet oscillating in the ($Y^0_3$) mode with a high external magnetic field $B_o$ =10 T. The radial flow is damped by the magnetic field, however the symmetry and continuity restrictions are not present here and the droplet continues to oscillate in the ($Y^0_3$) mode. The internal flow is quite different to the case without the magnetic field (Figure 5). In the presence of the strong DC magnetic field in the z-axis direction there is practically no radial flow, and the fluid oscillates in columns along the direction of the external magnetic field.

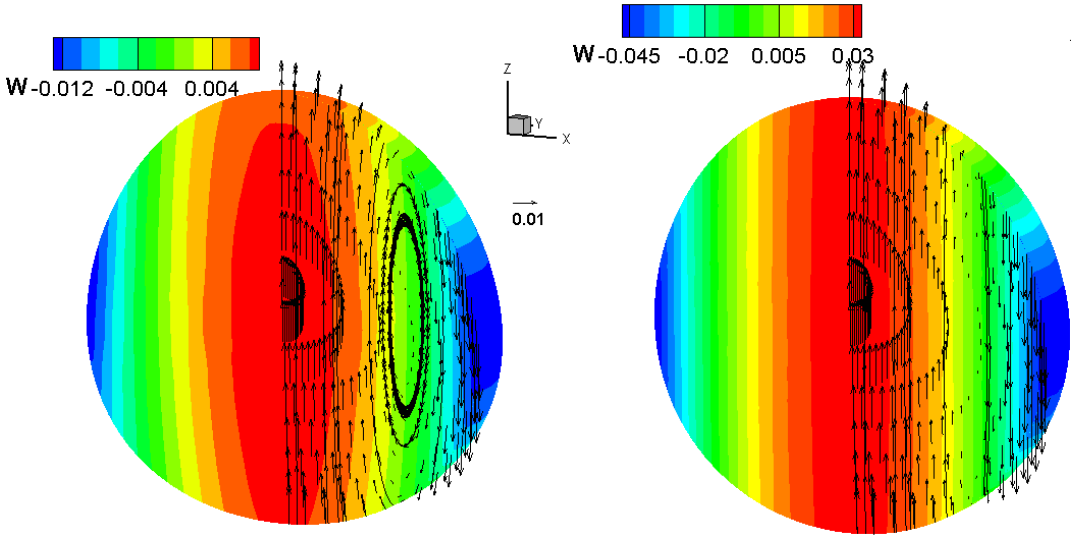


**Figure 4**. Oscillation mode (3,0) in $B_o$ =10 T magnetic field, velocity field at two moments: 0.226 s, and 0.232 s for the liquid Ni droplet.

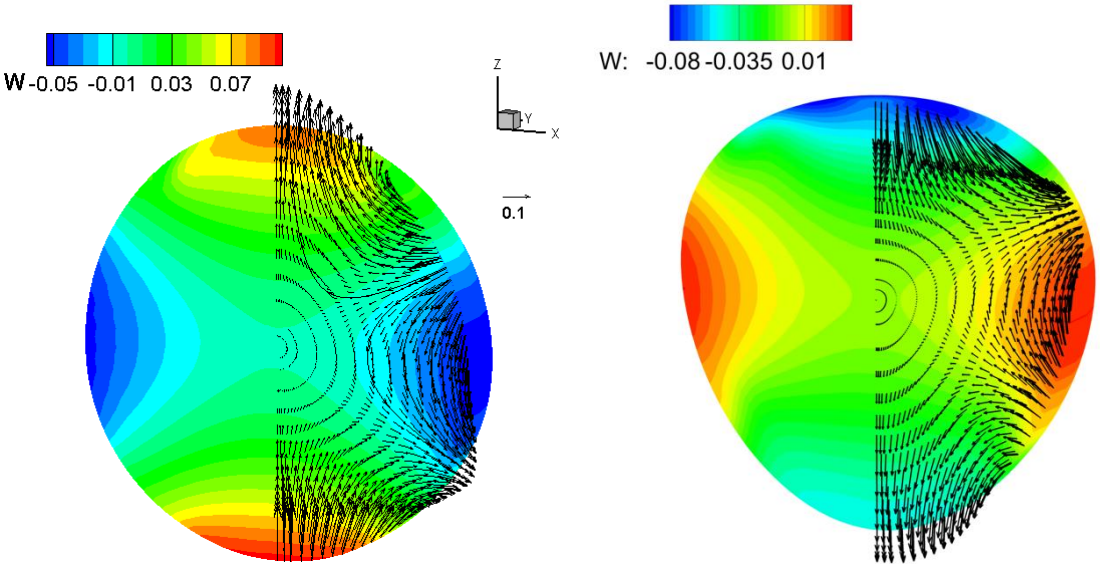


**Figure 5**. Oscillation Mode (3,0) without the magnetic field, velocity field at two moments for the liquid Ni droplet.

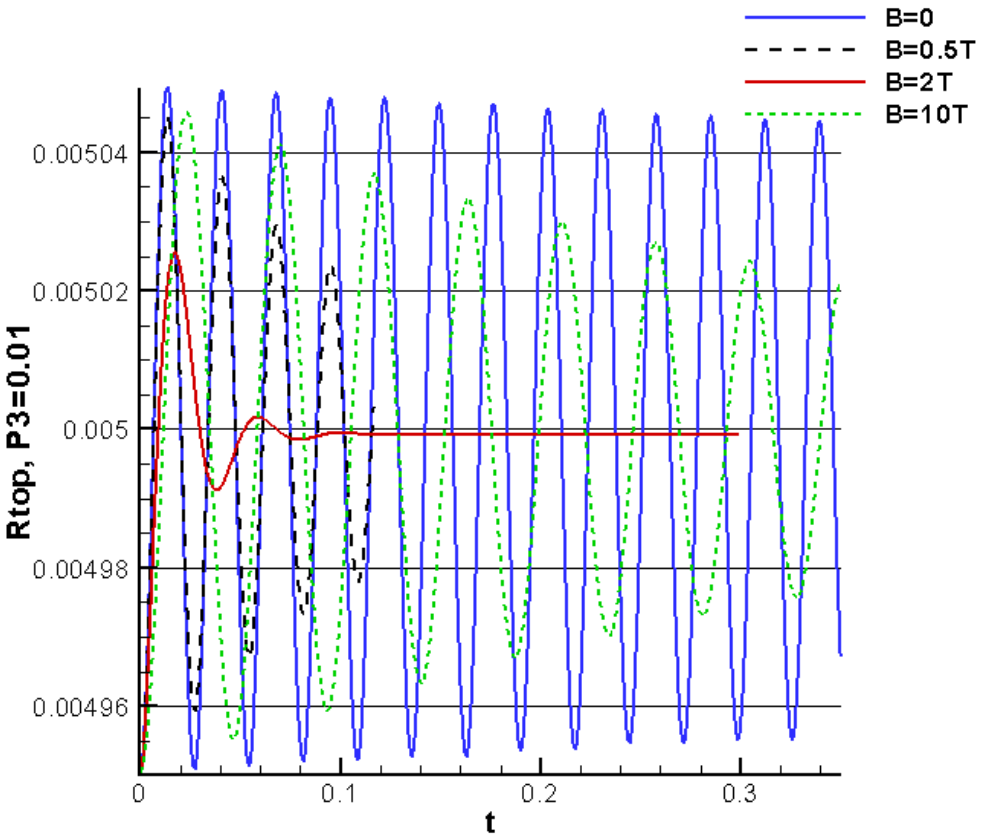


**Figure 6.** Oscillations of the top position for Ni droplet obtained in axisymmetric model for the (3,0) mode in different intensity uniform Bz field.

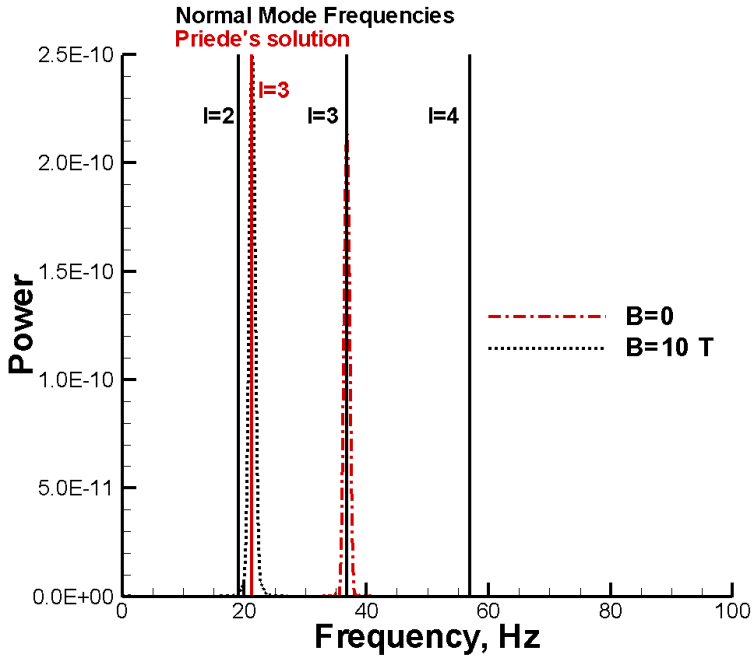


**Figure 7.** Spectra for the high magnetic field 10 T compared to the nonmagnetic case and the asymptotic solution [8] for the liquid Ni droplet.

It is of interest to investigate the oscillation change with the gradual increase of the magnetic field magnitude. Rayleigh normal mode frequency remains practically unchanged for a moderate magnetic field 0.5 T, however with the increased damping rate (Figure 6). Oscillations are close to overdamping at about 2 T. For extreme fields (10 T and more) the frequency gradually decreases to the asymptotic value given in [8]. We can conclude from these results that a DC field up to 0.5-1 T is beneficial to stabilize the oscillation, damp the turbulence while preserving the Rayleigh frequency. High DC fields (5 T and more) need updated models to interpret measurements. Figure 7 demonstrates that the asymptotic solution predicted frequency is achieved for the field of 10 T.

### 4.3. Freely Oscillating Droplets, Non-Axisymmetric Mode (2,1)

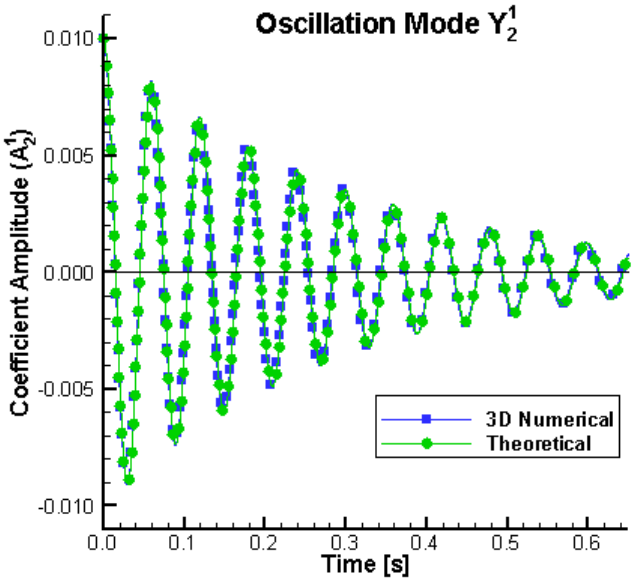


**Figure 8.** Time-Dependent Coefficient to ($Y^l_2$) mode.

The next case considered is the non-axisymmetric mode ($Y^l_2$), the droplet radius, amplitude, and magnetic field strength are for the Si droplet at 2.5 T. A volume correction is again made. Theoretical analysis shows that the oscillation frequency and the magnetic and viscous damping constants are given by:

$$\omega_2^1 = 2\sqrt{\frac{\Gamma}{\rho R_0^3}}, \tag{31}$$

$$\gamma_2^1 = 4\frac{\sigma B_0^2 R_0^3}{\Gamma} + \frac{5}{2}\frac{\nu}{R_0^2}, \tag{32}$$

Figure 8 shows the results of the 3D numerical simulation compared with the theoretical result. The two results show very good agreement. Figure 9 shows plots of the flow variables, flow for this mode only occurs in the x-z plane. It is clear from these contour plots that the surface oscillation mode is unchanged by the external magnetic field; however the internal flow has changed. The radial component of the flow is damped out and the fluid oscillates as columns along the direction of the magnetic field.

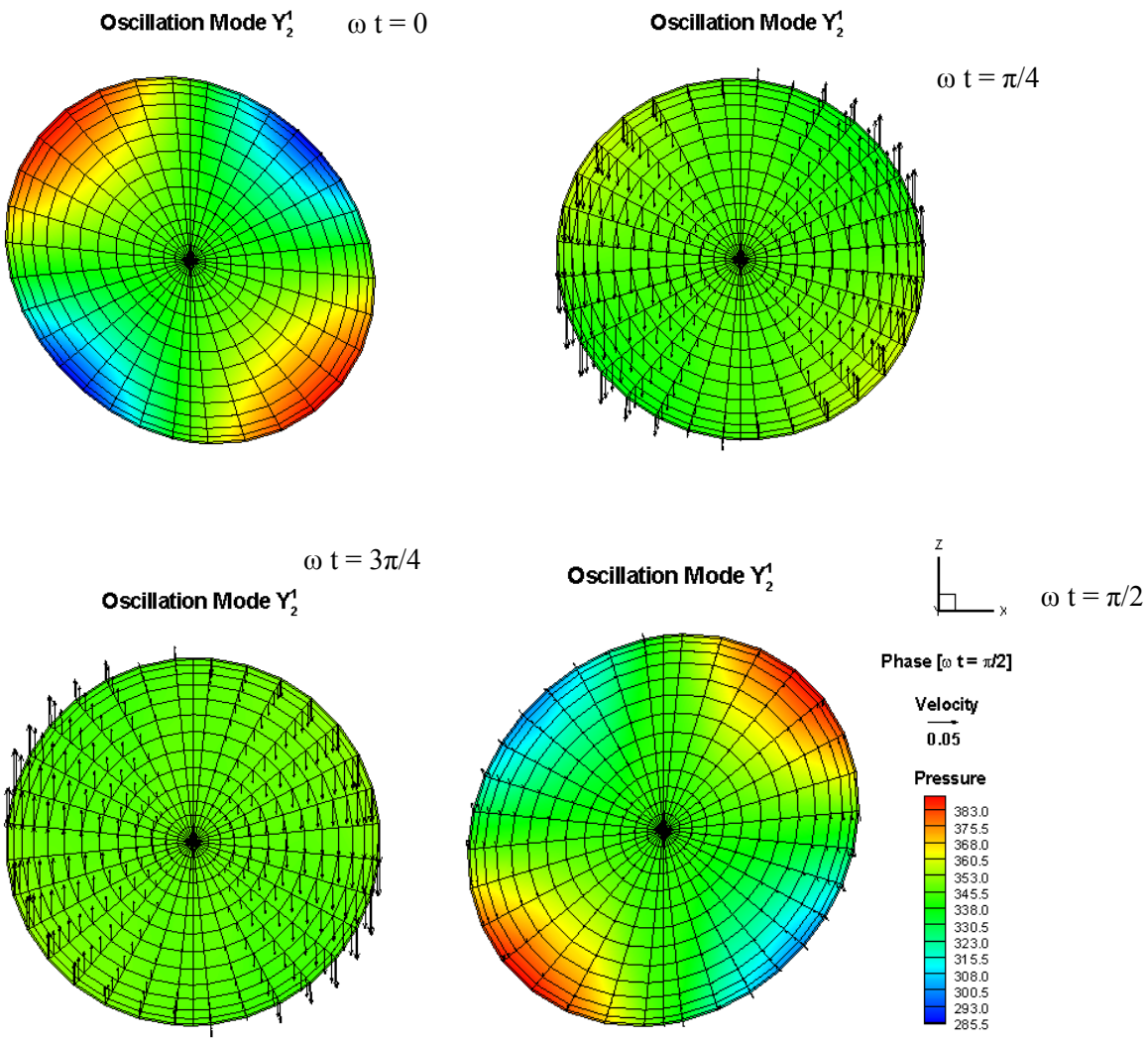


**Figure 9.** Oscillation mode (2,1), pressure contours and velocity vectors.

4.4. Freely Oscillating Droplets, Non-Axisymmetric Mode (2,2)

The next case considered is the non-axisymmetric mode ($Y^2_2$), the droplet radius, amplitude, and magnetic field strength are all the same as the previous case. A volume correction is again made. Theoretical analysis shows that the magnetic damping coefficient is zero and the oscillation frequency and viscous damping constant are the same as for the non-magnetic case:

$$\omega_2^2 = \sqrt{\frac{8\Gamma}{\rho R_0^3}}, \tag{33}$$

$$\gamma_2^2 = 0 + 5\frac{\nu}{R_0^2} \quad \text{(magnetic + viscous)}, \tag{34}$$

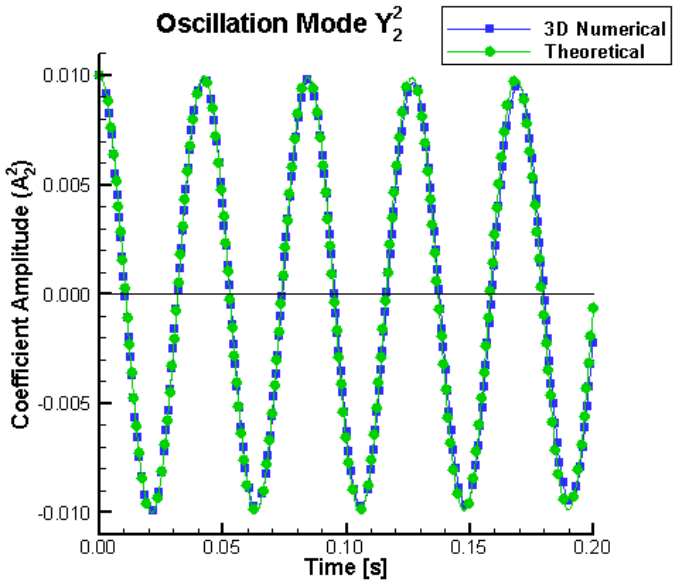


**Figure 10.** Time-Dependent Coefficient to ($Y^2_2$) mode.

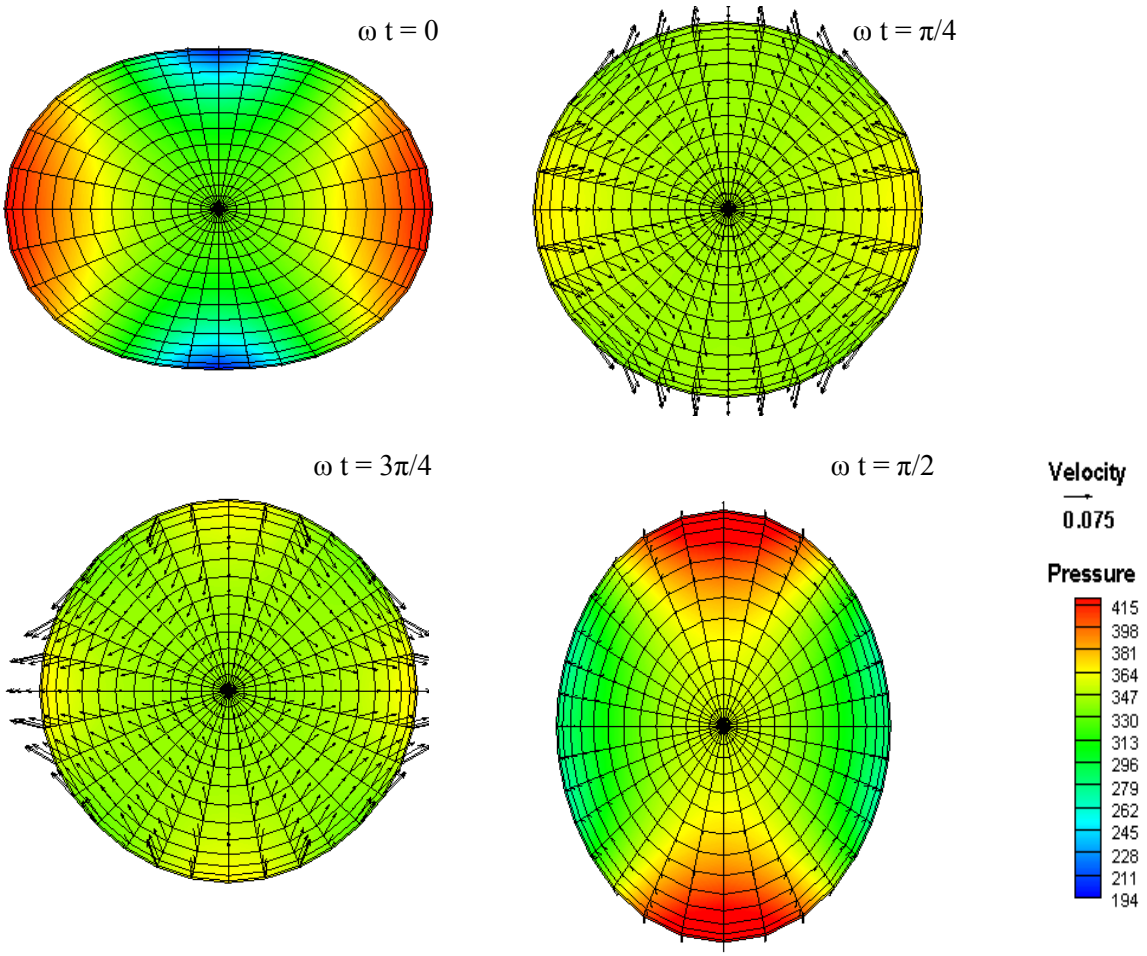


**Figure 11**. Oscillation mode (2,2), pressure contours and velocity vectors.

Figure 10 shows the results of the 3D numerical simulation compared with the theoretical result. The two results show very good agreement, the oscillation is unaffected by the external magnetic field. The reason for this behavior can be clearly understood from the plots of the fluid flow variables in Figure 11. Fluid flow for this mode only occurs in the x-y plane resulting in an electric field $(\boldsymbol{V} \times \boldsymbol{B})$ perpendicular to the flow but confined in the same plane. Due to the potential nature of the fluid flow, charge continuity cannot be satisfied and so an equal and opposite electric field $(-\nabla\phi)$ exists that results in zero net current and no damping of the flow by the Lorentz force.

## 5. Conclusions

The oscillating drop technique is a valuable method for measuring surface tension and viscosity of materials in a non-contact environment. Numerical results have been presented that confirm the asymptotic theoretical results relating surface tension and viscosity to frequency and damping rates for conducting droplets in a constant magnetic field. Further work involves use of the 3D numerical model to find qualitative and quantitative results for the oscillating drop technique in the presence of gravity forces. Comparison will also be made with experimental results where large amplitude and non-linear effects have a significant contribution to the dynamics and can impact on the measurement process.

## References

[1] Egry I, Lohofer G, Seyhan I, Schneider S and Feuerbacher B 1999 *Int. J. Thermophys*. **20** (4) 1005
[2] Cummings D L and Blackburn D A 1991 *J. Fluid Mech.* **224** 395
[3] Suryanarayana P V R and Bayazitoglu Y 1991 *Phys. Fluids* A **3** (5) 967
[4] Kobatake H, Fukuyama H, Minato I, Tsukada T and Avaji S 2007 *Applied Physics Letters* **90** 094102
[5] Bojarevics V, Easter S, Roy A and Pericleous K 2009 *Proc. Int. Symp.Liquid Metal Processing and Casting*, Santa Fe, TMS, ed-s Lee P, Mitchell A, Williamson R, 319
[6] Beaugnon E, Fabregue D, Billy D, Nappa J and Tournier R 2001 *Physica* B **294-295** 715
[7] Hill R J A and Eaves L 2010 *Phys. Rev* E **81 (**5) 056312
[8] Priede J 2010 *J. Fluid Mech.* **671** 399
[9] Lord Rayleigh 1879 *Proc. Royal Soc. London* A **29** 71
[10] Lamb H 1895 *Hydrodynamics*, Cambridge University Press, Cambridge
[11] Tsamopoulos J A and Brown R A 1983 *J. Fluid Mech.* **127** 519
[12] Smythe W R 1950, *Static and Dynamic Electricity*, McGraw-Hill, London
[13] Bojarevics V and Pericleous K 2003 *ISIJ International* **43** (6) 890